Progress In Electromagnetics Research C, Vol. 135, 83–94, 2023

Design and Analysis of a Compact 38 GHz Wideband Monopole Antenna for 5G mm-Wave Wireless Applications

Idrish Shaik[1, *] and Sahukara Krishna Veni[2]

Abstract—In the current system of wireless communication, users expect devices that are lightweight and offer broad bandwidth as well as a high data transmission rate. Developments in data speeds, bandwidth, ultra-low response times, excellent dependability, considerable accessibility, and improved device-to-device connectivity are what have driven wireless systems toward 5G. These 5G wireless systems require small and efficient antenna designs. This work proposes a 5G mm-wave quadrilateral slotted defected ground structure (QSDGS) including a wideband monopole antenna (WMA) for n259 and n260 5G mm-wave bands. Here, the DGS was modelled using two quadrilateral slots on a ground plane. An inset feeding technique and multiple slots were employed to patch. This structure consists of a DGS-loaded slotted antenna patch mounted on a Rogers/RT Duriod 5880 ($\varepsilon_r = 2.2$, loss tangent = 0.0009) with dimensions of $12 \times 11 \times 0.9\,\text{mm}^3$ ($1.42\lambda_g \times 1.30\lambda_g \times 0.10\lambda_g$). This embedded antenna radiating structure resonates from 35.5 GHz to 44.7 GHz, giving an impedance bandwidth of 9.2 GHz (24.2%), with a centre frequency of 38 GHz. 9.48 dB was the peak gain, and 83–94% efficiency was obtained over the wide band. Based on the extracted data from the proposed antenna, it was found that the antenna is capable of covering the 5G NR n259 and n260 with significant gain, bandwidth, and efficiency. Thus, the antenna has the ability to be considered a possible contender to be used in 5G wireless applications using mm-wave frequencies. A good agreement can be seen here between simulated and measured return losses.

1. INTRODUCTION

The fifth-generation (5G) network is expected to use the millimeter-wave frequency band, which would significantly increase the capacity of wireless technology [1]. In order to reach the significant capacity and throughput demands of future 5G networks, the spectrum now available at mm-wave frequencies is considered to be a likely choice [2]. Because of the rapidly increasing number of user devices, the necessity for bandwidth has also grown to accommodate the rising amount of data [3]. The number of electronic devices, such as high-definition televisions, video surveillance system, laptops, household appliances, sensors, wearable devices, cameras, and robotic systems is anticipated to surge in the near future. The data rate and bandwidth requirements for all these types of applications will be covered by 5G technology [4]. Therefore, it is believed that 5G wireless communication would be able to accommodate a numerous real-time application, tactile network [5], and systems that offer different degrees of quality (QoS) (such as broadband, latency, delay of packet) and view in terms of quality.

The most distinctive characteristics of 5G technologies are the relatively fast transmission of data, the avoidance of any delay, and the wider availability of connectivity. For highly populated urban regions where connection demand is strong, the 5G millimeter waves offers a compromise of penetration, coverage, speed, and capacity [6, 7].

Received 19 May 2023, Accepted 14 July 2023, Scheduled 27 July 2023

* Corresponding author: Idrish Shaik (idrishshaik@gmail.com).

[1] AU TDR-HUB, ECE Department, AU College of Engineering, Andhra University, Vishakhapatnam, India. [2] ECE Department, GVP College for Degree and PG Courses (Autonomous), Vishakhapatnam, India.

The implementation of sub-6 GHz and mm-wave frequencies presents additional hurdles for the fifth generation wireless antennas. The design of antennas for the 5G mm-wave frequencies that have been designated can be somewhat demanding for antenna designers. The mm-wave spectrum experiences increasing levels of loss due to propagation and the atmosphere [8]. Attenuation by the atmosphere will have a bigger effect on radio waves as their frequencies go up. The attenuation of signals in outer space is mostly due to atmospheric gas absorption. The mm-wave frequency band, which spans from 24 GHz to 80 GHz, has been recognized by the ITU (International Telecommunications Union) for the use in 5G technology. 28 GHz, 38 GHz, and 60 GHz are among the operating bands that mobile networks using 5G are taking into consideration. However, while the 28 GHz and 38 GHz bands are helpful for cellular networks, mobile communication systems with antenna configurations might have difficulties while tuning on the higher frequency bands [9]. Attenuation by the atmosphere will have a bigger effect on radio waves as their frequencies go up. The attenuation of signals in outer space is mostly due to atmospheric gas absorption.

A 4×4 multiple-input multiple-output (MIMO) antenna array was presented in [10]. This antenna has a 25–40 GHz bandwidth and 16 dBi gain. For high-gain dual-band applications, a small antenna for 28/38 GHz has been described. This antenna was developed in order to avoid the array's complexity as well as its enormous size in [11]. The pros of the co-planar waveguide slot antenna in [12] for 28/38 GHz, including its simple construction, efficient broadband performance, and low dispersion, were recently published. It was also suggested that a small, simple-geometry, broadband antenna could operate across 28 GHz, 38 GHz, or both [13, 14].

A MIMO antenna measuring $30 \times 35\,\text{mm}^2$ developed with DGS technology is presented in [15]. The gain of 8.6 dBi was accomplished, as well as bandwidth of 4 GHz, with the incorporation of the defective ground structure. A study that has been done in the field of mm-wave frequency has revealed that the overall size of the antenna should be relatively modest and that the spectrum should be considered an essential element in situations where there is substantial attenuation. Reports have shown that the devices in the industry or to be used in wireless systems have to be placed within devices that should be small in stature and have a wide frequency range and strong gain. Despite much investigation, there is still a dearth of high gains, as achieving such gains often requires either an array method or a significantly larger and more structurally sophisticated design. DGS has been utilized in the field of microstrip antennas in order to improve the radiation characteristics of the microstrip antenna by increasing the bandwidth and gain of the microstrip antenna, as well as suppressing higher mode harmonics and cross-polarization [16].

To overcome those challenges and meet the requirements of the 5G mm-wave spectrum, this proposed design offers a novel, less complex, small-scale, wide spectrum range, and high gain antenna with dimensions of $12 \times 11 \times 0.9\,\text{mm}^3$ with electrical dimensions of $1.42\lambda_g \times 1.30\lambda_g \times 0.10\lambda_g$ for 5G mm-wave applications. It resonates at 38 GHz and has a bandwidth of 9.2 GHz (35.5–44.7 GHz) with a peak gain of 9.47 dB making it suitable for broadband. The antenna presented in this work is made up of a patch with multiple slots which is mounted on a Rogers 5880 substrate with a quadrilateral slotted defected ground plane at the bottom. The structure of the paper is as follows. The design process for the antenna is covered in Section 2. The performance of the antenna is shown in Section 3 in relation to its physical features. The experiment's findings are presented in Section 4. Concluding evaluations are offered in the final section.

2. ANTENNA DESIGN METHODOLOGY

2.1. Geometry of Proposed Antenna

Figure 1 illustrates the antenna that has been proposed from both the top and bottom views. The numerically calculated antenna dimensions are $12 \times 11 \times 0.9\,\text{mm}^3$. The presented monopole is designed on an RT Duriod 5880 substrate which has a dielectric constant of 2.2, a loss tangent of 0.0009, and a thickness of 0.9 mm. The Rogers 5880 substrate was specifically chosen because of its low dielectric constant and ability to mitigate attenuations at higher frequencies. With using CST Studio Suite 2019, the designing, simulation, and evaluation of the structure are carried out. The ground is loaded with two quadrilateral slots and multiple slots in a patch. The excitation for the antenna is provided via a microstrip inset feed of $50\,\Omega$. This combination enables the antenna to cover a wide bandwidth, which

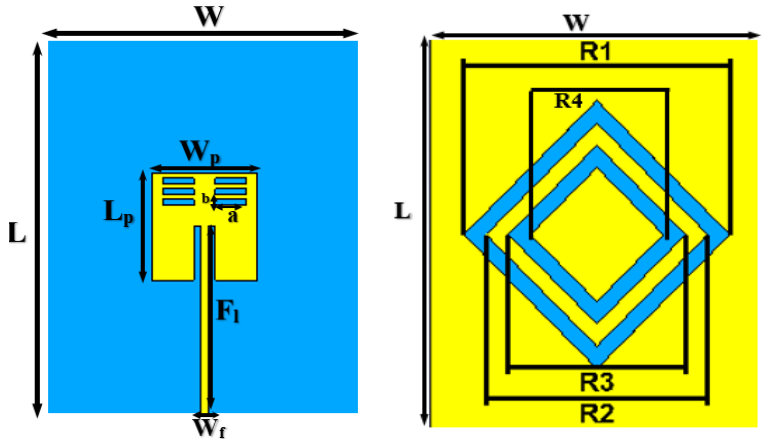

Figure 1. Proposed antenna. (a) Multiple slot patch. (b) Quadrilateral slotted ground plane.

ranges from 35.5 to 44.7 GHz. The following predefined design equations are used for calculating the antenna parameters [17].

Equation (1) [17] that follows can be applied in order to determine the width W_p of the patch

$$W_p = \frac{c}{2f_o}\sqrt{\frac{2}{\varepsilon_r+1}} = \frac{30}{2*38}\sqrt{\frac{2}{2.2+1}} = 0.311\,\text{cm (or) } 3.11\,\text{mm} \tag{1}$$

Equation (2) that is used to calculate the effective dielectric constant of the patch is [17]

$$\varepsilon_{reff} = \frac{\varepsilon_r+1}{2} + \frac{\varepsilon_r-1}{2}\left[1+12\frac{h}{W_p}\right]^{-\frac{1}{2}} \tag{2}$$

$$\varepsilon_{eff} = \frac{2.2+1}{2} + \frac{2.2-1}{2}\left[1+12\frac{0.09}{0.311}\right]^{-\frac{1}{2}} = 1.88$$

The extended incremental length of the patch can be calculated using the following Equation (3) [17]

$$\Delta L = 0.412h\frac{(\varepsilon_{reff}+0.3)\left(\frac{W_p}{h}+0.264\right)}{(\varepsilon_{reff}-0.258)\left(\frac{W_p}{h}+0.8\right)} \tag{3}$$

$$\Delta L = 0.412h\frac{(1.88+0.3)\left(\frac{0.311}{0.09}+0.264\right)}{(1.88-0.258)\left(\frac{0.311}{0.09}+0.8\right)} = 0.0434\,\text{cm (or) } 0.434\,\text{mm}$$

Through the use of Equation (4), the effective length of the patch may be determined [17]

$$L_{eff} = \frac{c}{2f\sqrt{\varepsilon_{reff}}} = \frac{30}{2*38\sqrt{1.88}} = 0.288\,\text{cm (or) } 2.88\,\text{mm} \tag{4}$$

By using Equation (5), the actual length of the patch, L_P, can be calculate [17]

$$L_p = L_{eff} - 2\Delta L = 0.288 - 2*0.0434 = 0.202\,\text{cm (or) } 2.02\,\text{mm} \tag{5}$$

The typical patch of the antenna that should resonate at 38 GHz should have dimensions of $3.1\times2\,\text{mm}^2$, according to the calculations given in the aforementioned Equations (1)–(5). However, the patch dimensions have been increased to $4\times4\,\text{mm}^2$ because of the compact design's difficulty to fabricate and

Table 1. Calculated numerical variables in design for the posited antenna in mm.

Parameter	L_p	W_p	L	W	F_l	W_f
Dimensions	4	4	12	11	10	1.5
Parameter	a	b	$R1$	$R2$	$R3$	$R4$
Dimensions	1.5	0.2	9	8	7	6

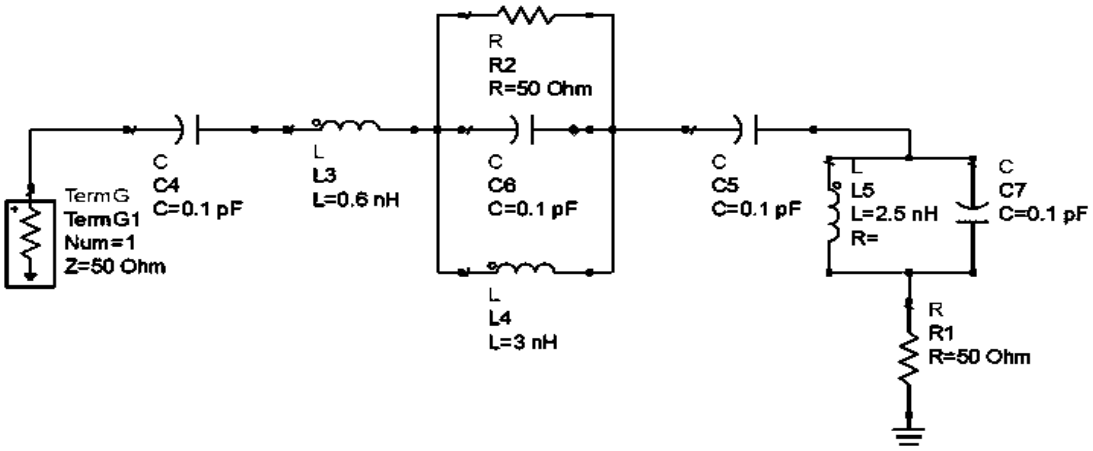

Figure 2. Equivalent circuit of the proposed antenna.

a need for a broad bandwidth. The suggested antenna has overall measurements of $12 \times 11 \times 0.9\,\text{mm}^3$ ($1.42\lambda \times 1.30\lambda \times 0.10\lambda$) listed in Table 1.

The equivalent circuit for the suggested design using RLC components is shown in Figure 2. Advanced Design System (ADS) software is used to design the circuit. In the equivalent circuit shown in Figure 2, low capacitance values were chosen, and as a result, precisely S-parameters were obtained that corresponded to those from the simulated design.

The return losses plots of the equivalent circuit and the proposed simulated S_{11} are shown in Figure 3. The impedance bandwidth is around 8.5 GHz, which is significantly smaller than the simulated impedance bandwidth, and the S_{11} reflection coefficient of the equivalent circuits is -16 dB at 39 GHz.

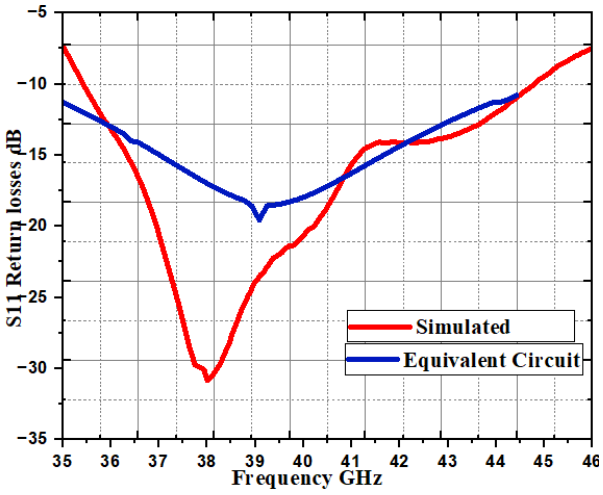

Figure 3. S_{11} return loss plot of equivalent circuit and simulated antenna.

From the observation, it is evident that the proposed antenna's power consumption is extremely low and has good significant characteristics.

2.2. Antenna Design Evolution Process

Figure 4 illustrates the evolution of the intended antenna and provides a step-by-step explanation of the technique. Based on the results, the antenna is in excellent condition for operation and uses the DGS mechanism to achieve broad band. Five antennas are presented here, with Antenna 1, Antenna 2, Antenna 3, and Antenna 4 representing the various phases of the development of the DGS loaded wideband antenna and Antenna 5 being the final presented antenna. Antenna 1 is a basic construction with a square patch, complete ground plane, and inset feeding, with dimensions expressed in Table 1. The 8 GHz bandwidth obtained from the primary construction of Antenna 1 can be seen in Figure 5(a). The ground plane of Antenna 2 shown in Figure 4(b) has been modified with a first quadrilateral slot of 9 mm radius that is inserted in accordance with the patch in the slot to increase the bandwidth by making electric fields concentrate in the center.

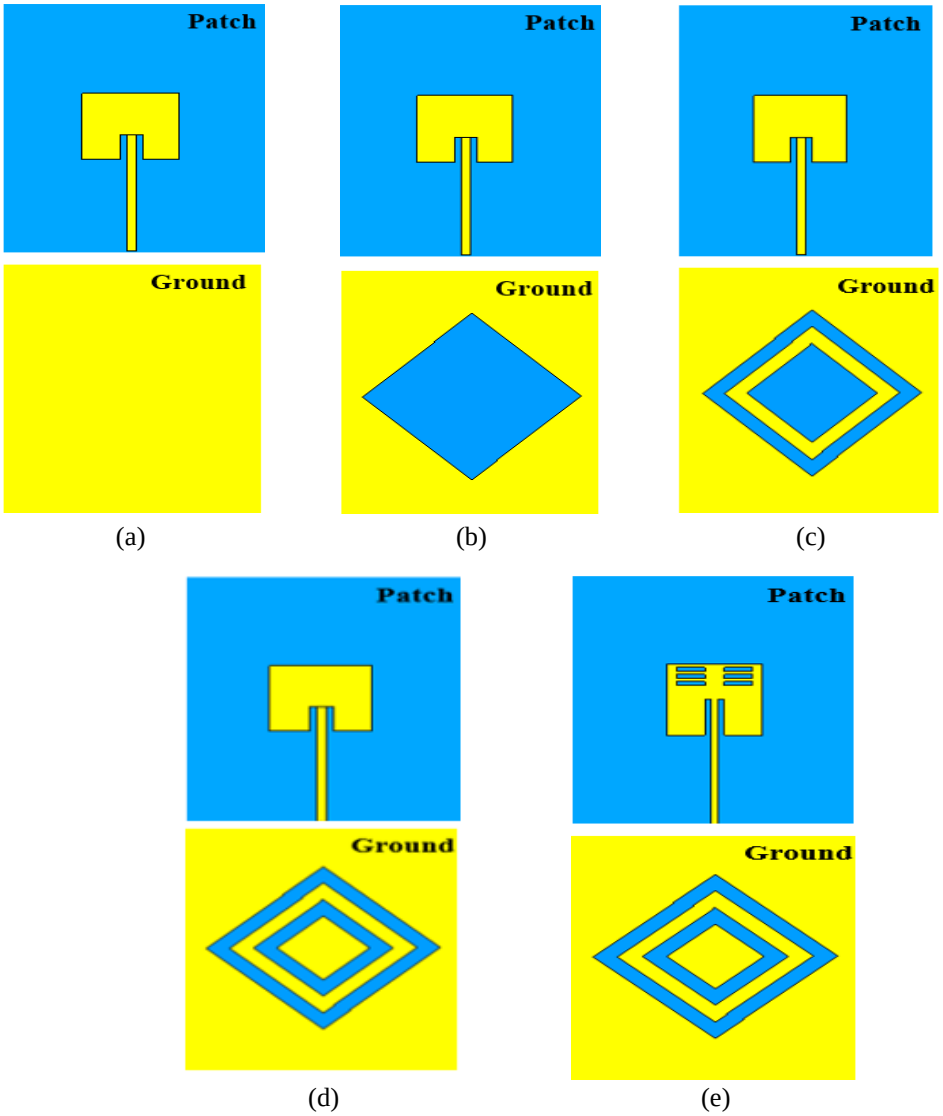

Figure 4. Various phases of antenna design evolution process. (a) Antenna-1, (b) Antenna-2, (c) Antenna-3, (d) Antenna-4, (e) Antenna-5.

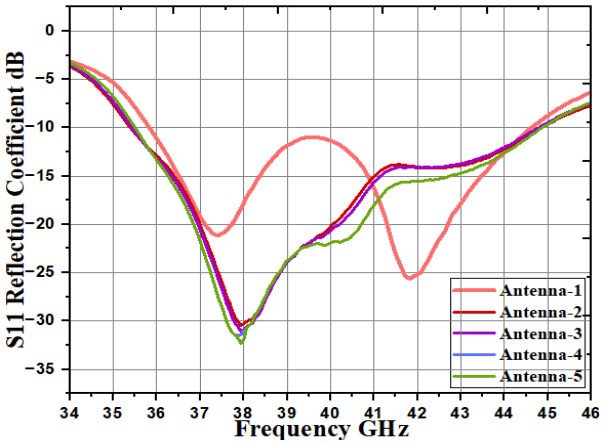

Figure 5. S_{11} return loss plot of various phases of antenna design evolution process.

The S_{11} plot in Figure 5 shows how this adjustment caused Antenna 2 to resonate at the 38 GHz desired frequency with a 9 GHz impedance bandwidth enhancement. Subsequently, Antenna 3 has now been improved by having quadrilateral slots inserted into the ground plane with 8 mm and 7 mm outer and inner radii, respectively. Figure 5 illustrates how this prompts the impedance bandwidth to increase to 9.1 GHz and the electric field to concentrate more in the center. The fourth antenna was modified with improving a fourth quadrilateral slot with a radius of 6 mm that was inserted into the ground plane to further enhance the bandwidth to 9.2 GHz with a return loss of −31 dB, and the final suggested antenna features the same three sets of slots on the left and right sides of the patch. To improve the return loss, these sets of slits are added in the patch, and from these changes the reflection coefficient improves more to −32 dB, as can be seen in Figure 5.

3. PARAMETRIC ANALYSIS

When four quadrilateral slots are put in the ground plane together with multiple sets of slots in the patch, the suggested antenna achieves wide band and high gain. Results were also seen when the slots were added in Figure 5. With the aid of the CST 2019 EM solver, four parameters, including patch $L_p \times W_p$ and slots in patches a and b, were examined for the parametric analysis by changing one parameter at a time while considering the other parameters constant.

3.1. Effect of Change in Dimensions of L_p and W_p

Figure 6(a) illustrates a plot of impedance bandwidth for a variety of combinations of L_p and W_p. $L_p = 4$ mm and $W_p = 4$ mm are two of the five values of L_p and W_p that are taken into consideration in this case. Figure 6(a) shows the difference in the S_{11} plot for the design of the rectangle with a size of $4 \times 4\,\text{mm}^2$.

3.2. Effect of Multiple Slots in Patch

The impact of the insertion of rectangular slots on the patch is seen in Figure 6(b). Here, three sets of identically sized slots on the left and right sides of the patch with the parameters $a = 1.5$ mm and $b = 0.5$ mm are selected for analysis. The reflection coefficient has been improved to −32 dB, demonstrating good results, and this was the main objective of having multiple sets of slots.

4. RESULTS WITH DISCUSSION

In this part, a detailed review of measured findings and the simulated results is presented, along with an analysis of the proposed antenna performance based on a variety of different performance measures.

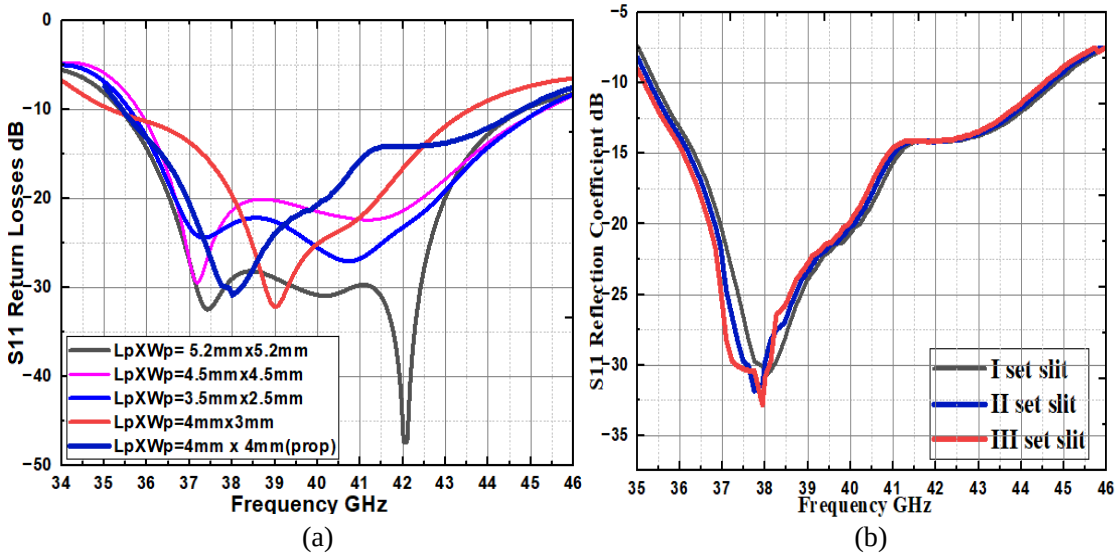

Figure 6. Effects on performance of antenna. (a) S_{11} plot due to Lp and Wp. (b) S_{11} plot due to slits in patch.

4.1. Reflection Coefficient

Figure 7 shows a plot of the computed and measured impedance spectrum values for the intended antenna. The proposed antenna design has a bandwidth of 9.2 GHz (24.2%), which allows it to cover a frequency band that ranges from 35.5 to 44.7 GHz. The proposed antenna was tested using a 2.42 SMA connector at VNA N5247A.09.90.02. The results from simulation and experiment are proven in good agreement and are suitable for the use in 5G applications.

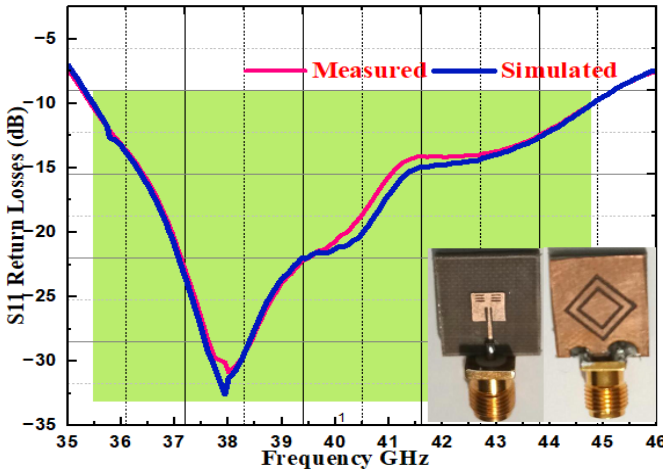

Figure 7. Simulated and experimented return loss S_{11} of proposed antenna.

4.2. Surface Current Distribution

The current excitation of the simulated antenna is shown and illustrated in Figure 8 which shows the antenna in operation at its resonant frequency of 38 GHz. Figures 8(a) and 8(b) clearly show that the current distribution could be seen at the inset feed and the defective ground structure.

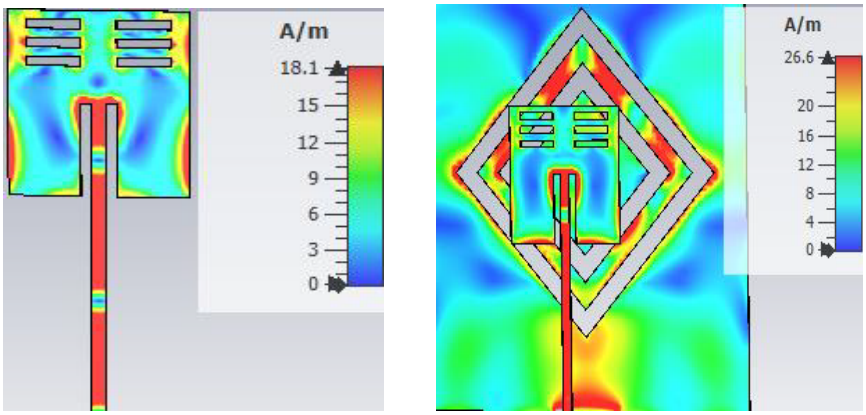

(a) (b)

Figure 8. (a) Current excitation of antenna at 38 GHz in patch. (b) Current excitation of antenna at 38 GHz in patch and ground.

4.3. Gain and Radiation Efficiency

Figure 9 provides an illustration of the proposed antenna's efficiency and gain. Figure 9(b) gives the minimum as well as maximum radiation efficiencies, which range from 83 to 94%. Figure 9(a) clearly shows the maximum gain of 9.48 dB at 35.5 GHz and 7.81 dB at resonating frequency of 38 GHz, and the overall gain obtained in the frequency range is more than 6.5 dB.

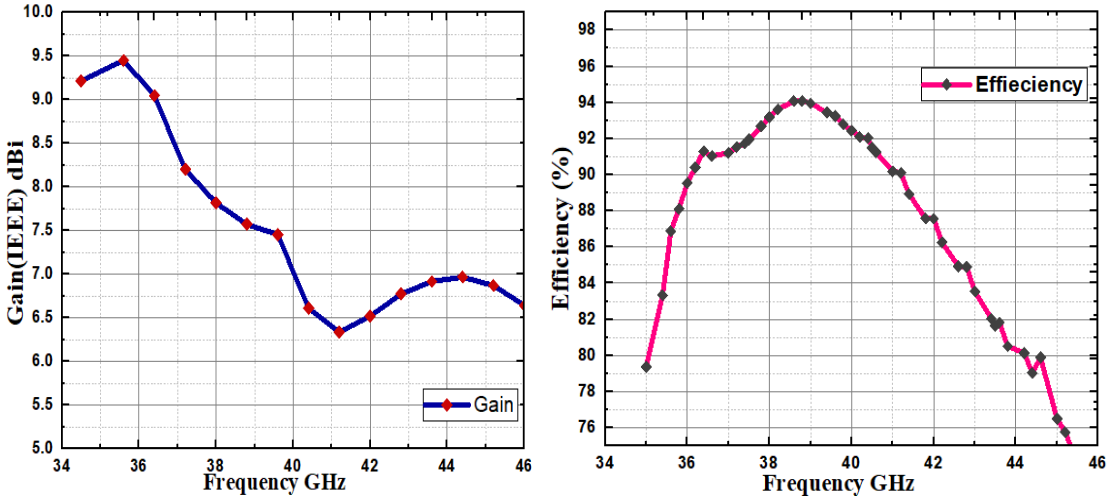

(a) (b)

Figure 9. (a) Gain (IEEE) plot vs frequency. (b) Efficiency plot vs frequency.

4.4. Characteristics of Electromagnetic Radiation

The three-dimensional gain plots of projected antenna structure are shown in Figures 10(a), (b), and (c) for the resonant frequencies of 35.5 GHz, 38 GHz, and 44.75 GHz. It is observed that from Figure 10(a) the peak gain of 9.48 dB was achieved, and 7.81 dB of gain was obtained at resonating frequency of 38 GHz shown in Figure 10(b). Figure 10(c) shows the 3D gain plot of 44.7 GHz with 6.81 dB. It is observed that that the gain was slightly decreased at higher frequencies, which may be due to attenuation at higher frequencies.

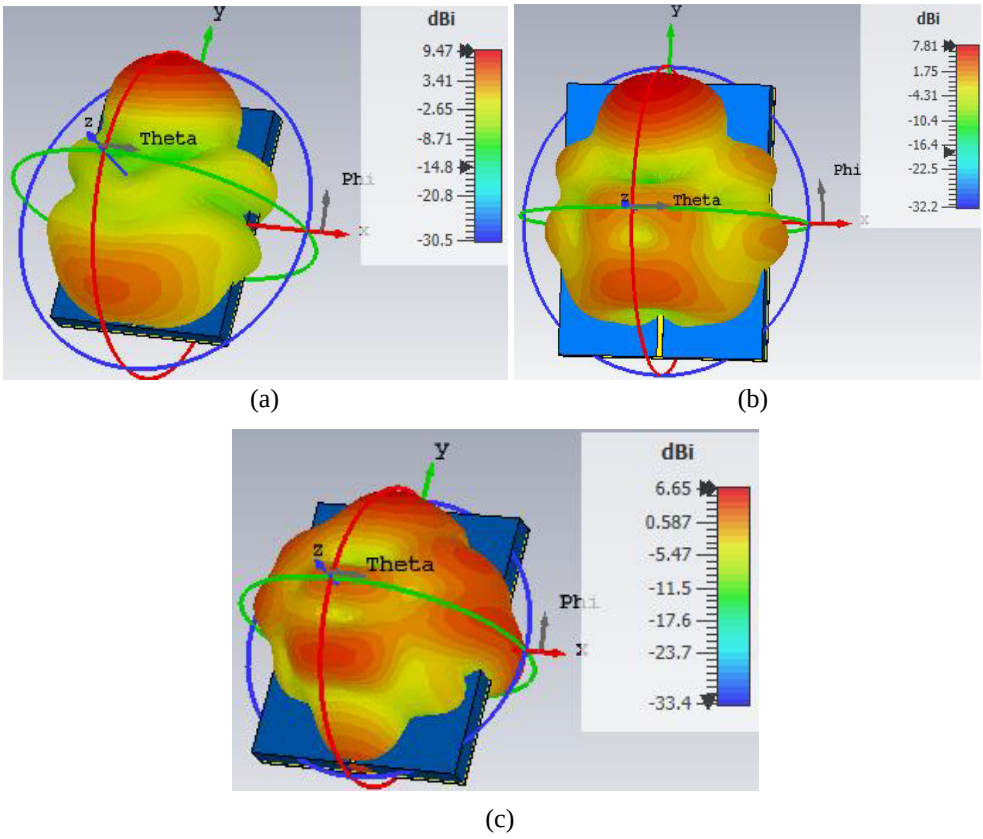

Figure 10. (a) 3D gain plot at 35.5 GHz. (b) 3D gain plot at 38 GHz. (c) 3D plot at 44.75 GHz.

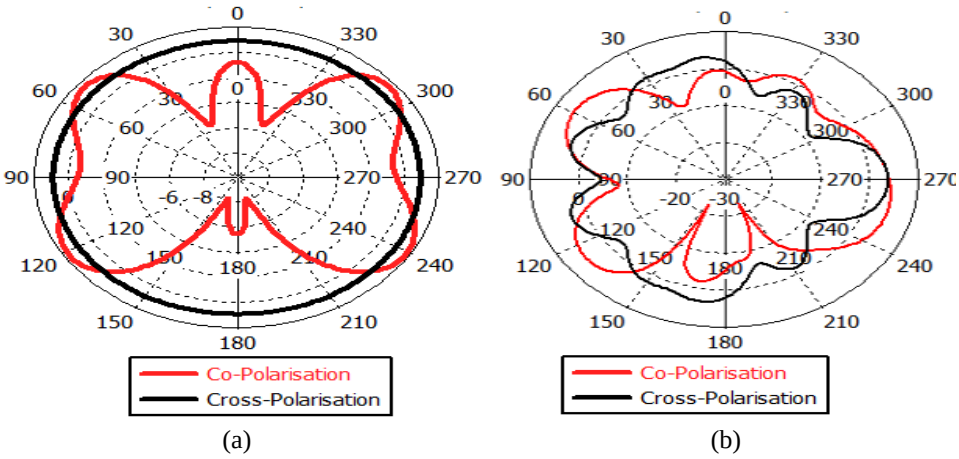

Figure 11. The pattern of radiation for proposed antenna at 38 GHz. (a) E plane, (b) H plane.

The pattern of radiation from the developed antenna design for the resonant frequency of 38 GHz is shown in Figure 11. The computed co-polarization and cross-polarization of two major planes give bi-directional patterns in the E-plane (XZ, $\emptyset = 0°$) shown in Figure 11(a) and omnidirectional patterns in the H-plane (YZ, $\emptyset = 90°$) in Figure 11(b).

The suggested antenna is modelled using CST 2019 software, and a Rogers 5880 is used to fabricate a prototype of the antenna for usage in practical applications. The top and bottom views of the fabricated element are shown in Figure 12.

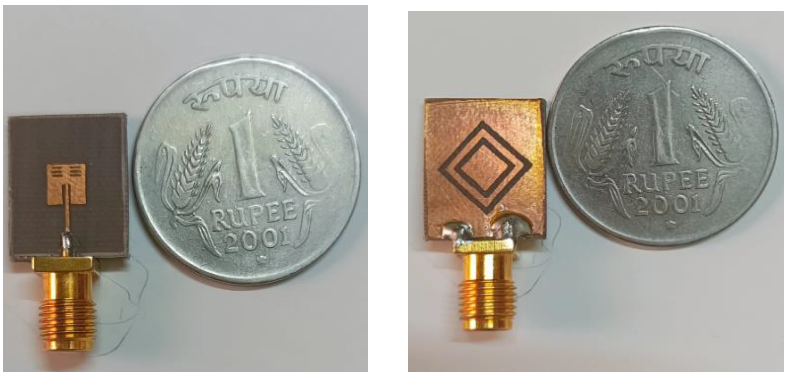

(a) (b)

Figure 12. (a) Top layer of the designed and fabricated antenna. (b) Bottom layer of the design and fabricated antenna.

4.5. Comparative Analysis

Table 2 compares the designed antenna to studies that have already been published in the recent past. The proposed antenna possesses beneficial radiation characteristics, including a wider bandwidth, steady gain, and high radiation efficiency. These characteristics give support to the concept that the design is acceptable with connection to systems of communication that operate within the millimeter wave spectrum.

Table 2. Comparison of proposed antenna results with previous works.

Ref.	Dimensions (λ^2)	Tuned frequency (GHz)	Bandwidth (GHz)	Gain (dB)	Radiation Efficiency (%)
[18], (2019)	1.30×1.12	28/38	2.6/2.1	1.27/1.83	78/76
[19], (2019)	0.56×0.56	28/45	1/3	7.6/7.21	85.6/95.3
[20], (2016)	3.8×2.7	26.5–38.3	11.8	15	90
[21], (2019)	0.21×0.10	27.5–40	12.5	7	75
[22], (2020)	7.4×7.4	23–40	12	12	75
[23], (2019)	5.13×10.27	28/38	2/2	7.95/8.27	89/88
[24], (2021)	2.34×0.99	27/39	3/5	5/5.7	99/98.6
[25], (2021)	1.86×2.24	28/38	1/1.2	7/7.9	85
[26], (2020)	1.12×2.37	28/37	6.3/3.9	7.1	70
[27], (2020)	1.0×1.0	24.5–31	6	9	95
[28], (2017)	2.80×1.40	38/73	4.6/8	2.9/3	90
[29], (2020)	1.92×3.20	38/60	6.5/5.5	2/2.2	89/79
[30], (2021)	1.48×1.48	37	6	8.25	98
Proposed	1.42×1.30	38	9.2	6.7–9.48	83–94

5. CONCLUSION

In order to obtain a broad bandwidth of 9.2 GHz, a small-scale, high-performance novel monopole antenna with a quadrilateral slotted defective ground has been thoroughly demonstrated. A multiple-slot patch and a slotted DGS are used in the design to provide a large bandwidth and the desired

resonant frequency. The design was implemented on a Rogers 5880 substrate, which has a centre frequency of 38 GHz, and it works significantly better than the antennas described in the previous works. Based on the results of both measured and simulated data, a significant reflection coefficient of −32 dB is obtained by the proposed antenna, which has a bandwidth of 9.2 GHz, a gain of more than 6.5 dB over the operating band, and a peak gain of 9.48 dB at 35.5 GHz. However, the gain is reduced at higher frequencies in the operating band. This is to be investigated, and we will explore this in our next work. The comparison of the proposed antenna to the previous work shows that the designed antenna is realistic for 5G mm-wave cellular applications like ultra HD multimedia, which require high data rates and bandwidth, especially in cellular infrastructure.

REFERENCES

1. Andrews, J. G., S. Buzzi, W. Choi, et al., "What will 5G be?" *IEEE Journal on Selected Areas in Communications*, Vol. 32, No. 6, 1065–1082, 2014, doi: 10.1109/jsac.2014.2328098.
2. Rappaport, T. S., S. Sun, R. Mayzus, et al., "Millimeter wave mobile communications for 5G cellular: It will work!," *IEEE Access*, Vol. 1, 335–349, 2013, doi: 10.1109/access.2013.2260813.
3. Cao, Y., K.-S. Chin, W. Che, W. Yang, and E. S. Li, "A compact 38 GHz multibeam antenna array with multifolded Butler matrix for 5G applications," *IEEE Antennas and Wireless Propagation Letters*, Vol. 16, 2996–2999, 2017, doi: 10.1109/lawp.2017.2757045.
4. Agyapong, P., M. Iwamura, D. Staehle, W. Kiess, and A. Benjebbour, "Design considerations for a 5G network architecture," *IEEE Communications Magazine*, Vol. 52, No. 11, 65–75, 2014, doi: 10.1109/mcom.2014.6957145.
5. Fettweis, G. and S. Alamouti, "5G: Personal mobile internet beyond what cellular did to telephony," *IEEE Communications Magazine*, Vol. 52, No. 2, 140–145, 2014, doi: 10.1109/mcom.2014.6736754.
6. Al-Gburi, A. J., Z. Zakaria, H. Alsariera, et al., "Broadband circular polarised printed antennas for indoor wireless communication systems: A comprehensive review," *Micromachines*, Vol. 13, No. 7, 1048, 2022, doi: 10.3390/mi13071048.
7. Yin, J., Q. Wu, C. Yu, H. Wang, and W. Hong, "Broadband endfiremagnetoelectric dipole antenna array using SICL feeding network for 5G millimeter-wave applications," *IEEE Transactions on Antennas and Propagation*, Vol. 67, No. 7, 4895–4900, 2019, doi: 10.1109/tap.2019.2916463.
8. Shayea, I., T. Abd Rahman, M. Hadri Azmi, and M. R. Islam, "Real measurement study for rain rate and rain attenuation conducted over 26 GHz microwave 5G link system in Malaysia," *IEEE Access*, Vol. 6, 19044–19064, 2018, doi: 10.1109/access.2018.2810855.
9. Zahra, H., W. A. Awan, W. A. E. Ali, N. Hussain, S. M. Abbas, and S. Mukhopadhyay, "A 28 GHz broadband helical inspired end-fire antenna and its MIMO configuration for 5G pattern diversity applications," *Electronics*, Vol. 10, No. 4, 405, Feb. 2021, doi: 10.3390/electronics10040405.
10. Sethi, W. T., M. A. Ashraf, A. Ragheb, A. Alasaad, and S. A. Alshebeili, "Demonstration of millimeter wave 5G setup employing high-gain Vivaldi array," *International Journal of Antennas and Propagation*, Vol. 2018, 1–12, 2018, doi: 10.1155/2018/3927153.
11. Jilani, S. F. and A. Alomainy, "A multiband millimeter-wave 2-D array based on enhanced Franklin antenna for 5G wireless systems," *IEEE Antennas and Wireless Propagation Letters*, Vol. 16, 2983–2986, 2017, doi: 10.1109/lawp.2017.2756560.
12. Ali, M. M. and A.-R. Sebak, "Dual band (28/38 GHz) CPW slot directive antenna for future 5G cellular applications," *2016 IEEE International Symposium on Antennas and Propagation (APSURSI)*, 2016, doi: 10.1109/aps.2016.7695908.
13. Przesmycki, R., M. Bugaj, and L. Nowosielski, "Broadband microstrip antenna for 5G wireless systems operating at 28 GHz," *Electronics*, Vol. 10, No. 1, 1, 2020, doi: 10.3390/electronics10010001.
14. Hussain, M., S. M. R. Jarchavi, S. I. Naqvi, et al., "Design and fabrication of a printed tri-band antenna for 5G applications operating across Ka- and V-band spectrums," *Electronics*, Vol. 10, No. 21, 2674, 2021, doi: 10.3390/electronics10212674.

15. Khalid, M., S. I. Naqvi, N. Hussain, M. U. Rahman, and Y. Amin, "4-port MIMO antenna with defected ground structure for 5G millimeter wave applications," *Electronics*, Vol. 9, No. 1, 71, 2020, doi: 10.3390/electronics9010071.
16. Khandelwal, M. K., B. K. Kanaujia, and S. Kumar, "Defected ground structure: Fundamentals, analysis, and applications in modern wireless trends," *International Journal of Antennas and Propagation*, Vol. 2017, 1–23, 2017, doi: org/10.1155/2017/2018527.
17. Shaik, I. and S. K. Veni, "A novel quadrangular slotted DGS with a wideband monopole radiator for fifth-generation sub-6 GHz mid-band applications," *Progress In Electromagnetics Research C*, Vol. 133, 109–120, 2023.
18. Hasan, Md. N., S. Bashir, and S. Chu, "Dual band omnidirectional millimeter wave antenna for 5G communications," *Journal of Electromagnetic Waves and Applications*, Vol. 33, No. 12, 1581–1590, 2019, doi: 10.1080/09205071.2019.1617790.
19. Khattak, M. I., A. Sohail, U. Khan, Z. Barki, and G. Witjaksono, "Elliptical slot circular patch antenna array with dual band behaviour for future 5G mobile communication networks," *Progress In Electromagnetics Research C*, Vol. 89, 133–147, 2019.
20. Dadgarpour, A., M. S. Sorkherizi, and A. Kishk, "A wideband low loss magneto electric dipole antenna for 5G wireless network with gain enhancement using meta lens and gap waveguide technology feeding," *IEEE Transactions on Antennas and Propagation*, Vol. 64, No. 12, 5094–5101, 2016, doi: 10.1109/TAP.2016.2620522.
21. Al Abbas, E., M. Ikram, and A. T. Mobashsher, "MIMO antenna system for multi-band millimeter-wave 5G and wideband 4G mobile communications," *IEEE Access*, Vol. 7, 181916–181923, 2019, doi: 10.1109/ACCESS.2019.2958897.
22. Sehrai, D. A., M. Abdullah, A. Altaf, S. H. Kiani, F. Muhammad, M. Tufail, M. Irfan, A. Glowacz, and S. Rahman, "A novel high gain wideband MIMO antenna for 5G millimeter wave applications," *Electronics*, Vol. 9, 1031, 2020, doi: 10.3390/electronics9061031.
23. Marzouk, H. M., M. I. Ahmed, and A. H. A. Shaalan, "Novel dual-band 28/38 GHz MIMO antennas for 5G mobile applications," *Progress In Electromagnetics Research C*, Vol. 93, 103–117, 2019.
24. Ali, W., S. Das, H. Medkour, and S. Lakrit, "Planar dual-band 27/39 GHz millimeter-wave MIMO antenna for 5G applications," *Microsyst. Technol.*, Vol. 27, No. 1, 283–292, 2021, doi: 10.1007/s00542-020-04951-1.
25. Raheel, K., A. Altaf, A. Waheed, S. H. Kiani, D. A. Sehrai, F. Tubbal, and R. Raad, "E-shaped H-slotted dual bandmm wave antenna for 5G technology," *Electronics*, Vol. 10, 1019, 2021, doi: 10.3390/electronics10091019.
26. Venkateswara Rao, M., B. T. Madhav, J. Krishna, Y. Usha Devi, T. Anilkumar, and B. Prudhvi Nadh, "CSRR-loaded T-shaped MIMO antenna for 5G cellular networks and vehicular communications," *International Journal of RF and Microwave Computer-Aided Engineering*, Vol. 29, No. 8, e21799, 2020, doi: 10.1002/mmce.21799.
27. Hussain, N., M. J. Jeong, A. Abbas, and N. Kim, "Metasurface-based single-layer wideband circularly polarized MIMO antenna for 5G millimeter-wave systems," *IEEE Access*, Vol. 8, 130293–130304, 2020, doi: 10.1109/access.2020.3009380.
28. Li, S., T. Chi, and Y. Wang, "A millimeter-wave dual-feed square loop antenna for 5G communications," *IEEE Transactions on Antennas and Propagation*, Vol. 65, No. 12, 6317–6328, 2017, doi: 10.1109/tap.2017.2723920.
29. Sharaf, M. H., A. I. Zaki, R. K. Hamad, and M. M. M. Omar, "A novel dual-band (38/60 GHz) patch antenna for 5G mobile handsets," *Sensors*, Vol. 20, No. 9, 2541, Apr. 2020, doi: 10.3390/s20092541.
30. Shamim, S. M., U. S. Dina, N. Arafin, and S. Sultana, "Design of efficient 37 GHz millimeter wave microstrip patch antenna for 5G mobile application," *Plasmonics*, Vol. 16, No. 4, 1417–1425, 2021, doi: 10.1007/s11468-021-01412-x.